MEDICAL SCIENCE MONITOR

CLINICAL RESEARCH

e-ISSN 1643-3750
© Med Sci Monit, 2021; 27: e932410
DOI: 10.12659/MSM.932410

Received: 2021.03.26
Accepted: 2021.06.28
Available online: 2021.07.16
Published: 2021.10.13

# Comparing the Traditional Versus Conservative Endodontic Access Cavities Design of the Maxillary First Molar: Using Cone-Beam Computed Tomography

Authors' Contribution:
Study Design A
Data Collection B
Statistical Analysis C
Data Interpretation D
Manuscript Preparation E
Literature Search F
Funds Collection G

ABE 1 Huachao Sui*
ABE 2 Bo Zhao*
BE 1 Haidan Nie*
BG 1 Xin Hao
C 3 Feng Qiao
C 1 Cuicui Sun
G 4 Changyi Li
E 1 Liwen Zhou
AG 1 Ligeng Wu

1 Department of Endodontics, College of Stomatology, Tianjin Medical University, Tianjin, PR China
2 Department of Stomatology, The First Hospital of Jilin University, Changchun, Jilin, PR China
3 Department of Maxillofacial Surgery, College of Stomatology Tianjin Medical University, Tianjin, PR China
4 School of Stomatology, Tianjin Medical University, Tianjin, PR China

* Huachao Sui, Bo Zhao, and Haidan Nie contributed equally to this work

**Corresponding Author:** Ligeng Wu, e-mail: lwu06@tmu.edu.cn
**Financial support:** Research Plan of Undergraduate Teaching Quality and Teaching Reform in Tianjin Ordinary Colleges and Universities, Tianjin [grant number B201006204]

**Background:** This study aimed to compare the size and location of the traditional and conservative endodontic access cavities of the right maxillary first molar teeth, projected on the occlusal surface using cone-beam computed tomography (CBCT), to obtain an ideal access cavity.

**Material/Methods:** Five hundred CBCT images of the right maxillary first molars, including 198 males and 302 females, were retrospectively evaluated using KaVo eXam Vision software. First, a rectangular coordinate system was established. The coordinates of 4 pulp horns and 3 root canal orifices, which projected on the occlusal surface, were marked on it. Two different access cavities were then created by connecting these points: (1) traditional endodontic access cavity (TEC) required removal of the entire roof of the pulp chamber to establish a straight-line access to the root canal system; (2) conservative endodontic access cavity (CEC) was formed by connecting the projection of each root canal orifice on the occlusal. Data were analyzed using Kruskal-Wallis and Pearson's correlation tests at a 5% significance level.

**Results:** The area of TEC was approximately 9.61 $mm^2$ for males and 8.91 $mm^2$ for females. The area of CEC was approximately 3.4 $mm^2$ for males and 3.16 $mm^2$ for females. The projections of all pulp horns and root canal orifices were in or near the central area of nine-rectangle-grid.

**Conclusions:** Compared with the traditional access cavity, creating a conservative access cavity was less invasive. Meanwhile, the access cavity should be limited to the central or near the central area of nine-rectangle-grid.

**Keywords:** Cone-Beam Computed Tomography • Dental Cavity Preparation • Dental Pulp Cavity • Molar

**Full-text PDF:** https://www.medscimonit.com/abstract/index/idArt/932410







Indexed in: [Current Contents/Clinical Medicine] [SCI Expanded] [ISI Alerting System] [ISI Journals Master List] [Index Medicus/MEDLINE] [EMBASE/Excerpta Medica] [Chemical Abstracts/CAS]

## Background

The maxillary first permanent molar erupts early and is key to mastication. Hence, pulpal and periapical diseases are common, and they frequently require endodontic treatment. Straight-line access from the pulp chamber to the root canal system is typically used in conventional root canal therapy. However, this usually results in excessive removal of tooth tissue [1], which can weaken the rigidity of the tooth [2] and decrease its fracture resistance [3]. Excessively large and improperly located endodontic access cavities are the primary reasons for loss of tooth structure [4,5].

The traditional endodontic access cavity (TEC) involves removing the entire roof of the pulp chamber and all cervical dentin to obtain a straight-line pathway to all canal orifices. Infected and necrotic tissues are also removed [6]. Recently, the concept of conservative endodontic access cavity (CEC), with the goal of minimally invasive dentistry [3,7], has been developed to preserve the tooth's structural integrity by saving pericervical dentin as much as possible [8]. The use of a conservative access cavity allows the retention of more dental tissue, including part of the pulp chamber roof and cervical dentin [9-13]. However, the location and size of pulp horns (that guide the TEC) and root canal orifices (that guide the CEC) projected on the occlusal surface are unclear.

An *in vitro* study showed the relationship between the coronal access outline on the occlusal surface and the root canal orifices in molars. The occlusal surfaces and the exposed root canal orifices were photographed, after which the pre- and post-sectioning images of each specimen were stacked [14]. In another study with 55 extracted mandibular second molars, the localization and distribution of the root canal orifices was evaluated using digital photography and image stacking [15]. However, the image stacking technique is extremely sensitive, and image magnification often causes distortion, making it difficult to obtain accurate measurements of the anatomical position of the root canal orifices. Nowadays, CBCT is used as a three-dimensional (3D) imaging tool for in vivo data measurement, which can accurately identify the root canal orifices' position at the pulp chamber floor and accurately display the anatomical structure of the tooth [16].

Cone-beam computed tomography (CBCT) is a commonly used diagnostic tool in dentistry. CBCT images can illustrate the internal structures of teeth three-dimensionally and accurately at a high resolution while simultaneously eliminating the problem of superimposing anatomical structures by combining sagittal, coronal, and axial CBCT images [17,18]. It is used extensively in in vivo dental anatomy studies and clinical applications, mainly related to root canal systems [19,20]. It has also been used to acquire the precise pulp chamber landmark measurements in molars [21].

This study aimed to compare 2 endodontic access cavities of the maxillary first molar by contrasting the location and size of CBCT-derived designs of pulp horn projections and root canal orifice projections onto the occlusal surface, for obtaining ideal endodontic access cavities, retaining more healthy dental tissue, accurate positioning and controlling the coronal access cavity, and providing anatomic evidence for clinicians to standardize access opening, especially for the posterior teeth.

## Material and Methods

### Subjects

This study was approved by the Ethics Committee of the Stomatological Hospital of Tianjin Medical University (TMUhMEC2019015). Five hundred digitized CBCT images were selected for retrospective analysis in the Department of Radiology, Stomatological Hospital, Tianjin Medical University. These images were obtained when patients visited the hospital for an implant or orthodontic treatment between 2015 and 2018.

The inclusion criteria were: patient's age between 10 and 70 years; right maxillary first molars with an intact crown; no open apices, caries, periapical lesions, restorations, or root fractures; no intraradicular restorations, posts, metallic restorations, or other types of fixed prostheses; no calcification; and good image quality.

### Cone-Beam Computed Tomographic Scans

CBCT images were taken using a KaVo 3D eXam device (Imaging Sciences International, Hatfield, PA) operated at 120 kV, 5 mA. Other scan parameters were: voxel size, 0.25 mm, field-of-view, 208 $cm^2$ (16×13 cm), and exposure time, 0.4 seconds. Scans were performed according to the manufacturer's instructions. All images were analyzed in a dark room using a tablet with a 1920×1080 pixels resolution. The contrast and brightness of the images were adjusted to ensure the best visual effect.

### Determination of Baseline Plane on the CBCT Images Before Measurement

The coronal (blue line), sagittal (green line), and axial planes (red line) were positioned on the right maxillary first molar on a CBCT image (**Figure 1**) and the baseline plane was established. The longitudinal axis of the target tooth was adjusted to be perpendicular to the axial plane (horizontal plane). The tooth was rotated on the sagittal plane to ensure that the longitudinal axis of the tooth was without a mesial-distal tilt (**Figure 1B**). The coronal plane was also rotated so that the longitudinal axis of the tooth was without a buccal-lingual tilt (**Figure 1C**). After that, we combined the coronal plane with the





Indexed in: [Current Contents/Clinical Medicine] [SCI Expanded] [ISI Alerting System] [ISI Journals Master List] [Index Medicus/MEDLINE] [EMBASE/Excerpta Medica] [Chemical Abstracts/CAS]


**Figure 1.** Cone-beam computed tomography images identifying the baseline plane of a right maxillary first molar for subsequent measurements of anatomical landmarks. (**A**) The axial plane view shows that the blue line has been adjusted to be parallel to the mesial and distal crown margin tangential line and bisects the baseline plane. Similarly, the green line has been adjusted to be parallel to the buccal and lingual crown margin tangential line and bisects the baseline plane. (**B**) The sagittal plane view shows that the tooth has no mesial-distal tilt. This was achieved by adjusting the longitudinal axis of the target tooth parallel to the blue line. (**C**) The coronal plane view shows that the tooth has no buccal-lingual tilt. This was also achieved by adjusting the longitudinal axis of the target tooth parallel to the green line.

sagittal plane, moving the red line, across the dentin-enamel junction, to the dentin (**Figure 1B, 1C**). Next, we moved the green line and the blue line on the axial plane, ensuring that the green line was parallel to the mesial-distal direction and bisected the buccal-lingual distance and that the blue line was parallel to the buccal-lingual direction and bisected the mesial-distal distance on the axial plane. The intersection of the above 2 lines was placed at the center of the crown (**Figure 1A**).

The axial plane view was amplified to decrease the measurement error by adjusting the length of the bottom of the axial plane view to 65 mm (13×5×1 mm=65 mm). Finally, 4 tangents were drawn at the 4 crown margin lines of the right maxillary first molar, on the axial plane view. The axial plane was defined as the baseline plane (**Figure 2A**).

### Establishment of a Rectangular Coordinate System After Determining the Baseline Plane

The X-axis was set as the mesial crown margin tangential line and the Y-axis was set as the buccal crown margin tangential line, to establish a rectangular coordinate system for subsequent measurements of pulp horns and root canal orifices on the baseline plane (**Figure 2A**). All measurements of location and size of projections of pulp horns and root canal orifices on the occlusal surface were taken using this rectangular coordinate system from the axial plane view on CBCT images.

### Measurement of Pulp Horn Projections on CBCT Images

Moving the red axial plane line slowly toward the root on the rectangular coordinate system, a low-density image of the mesiobuccal (MB) pulp horn appeared on the baseline plane, and the coordinates were marked ($x_1$, $y_1$). The line was moved further toward the root until the low-density image of the distobuccal (DB), mesiopalatal (MP), and distopalatal (DP) pulp horns appeared. Each of their coordinates was also marked ([$x_2$, $y_2$], [$x_3$, $y_3$], and [$x_4$, $y_4$], respectively) (**Figure 2B-2E**).

### Measurement of Root Canal Orifice Projections on CBCT images

When the red axial plane line was continuously moved toward the root until the image showed the high-density shadow of the pulp floor, three low-density shadows of the 3 root canal orifices (MB, DB, and palatal) appeared. The position of each root canal orifice was on the center point of the low-density shadow. The coordinates of the 3 root canal orifices were marked ([$x_5$, $y_5$], [$x_6$, $y_6$], and [$x_7$, $y_7$], respectively) (**Figure 2F-2H**).

Thus, 8 coordinates were obtained for each CBCT image (**Table 1**): the first measurement was the intersection of the palatal tangent line and the distal tangent line ($x_0$, $y_0$) (**Figure 2A**), while the remaining 7 coordinates reflected the positions of 4 pulp horns ([$x_1$, $y_1$], [$x_2$, $y_2$], [$x_3$, $y_3$], and [$x_4$, $y_4$]), and 3 root canal orifices ([$x_5$, $y_5$], [$x_6$, $y_6$], [$x_7$, $y_7$]) (**Figure 2B-2H**). The 8 coordinate points were measured 3 times to yield their average, and this was corrected to 0.01 mm.

### Observers

Two endodontic graduate students (A and B) received standardized training on KaVo 3D eXam Vision software by a radiologist with 20 years of clinical experience, to ensure accurate identification and measurement of anatomical landmarks in the CBCT images. First, all 3 independently examined 20 CBCT images where each CBCT image had 8 coordinate points (16 data points), yielding 16×20=320 measurements. One week later, the 2 endodontic graduate students repeated the 320 measurements. Before starting the study, the intra- and inter-observer agreements between the radiologist and students A and B were calculated using the interclass correlation coefficient (ICC) to evaluate data reliability. According to the standardized measurement procedure mentioned above, the 2 endodontic graduate students measured 500 CBCT images for the study.





Indexed in: [Current Contents/Clinical Medicine] [SCI Expanded] [ISI Alerting System] [ISI Journals Master List] [Index Medicus/MEDLINE] [EMBASE/Excerpta Medica] [Chemical Abstracts/CAS]

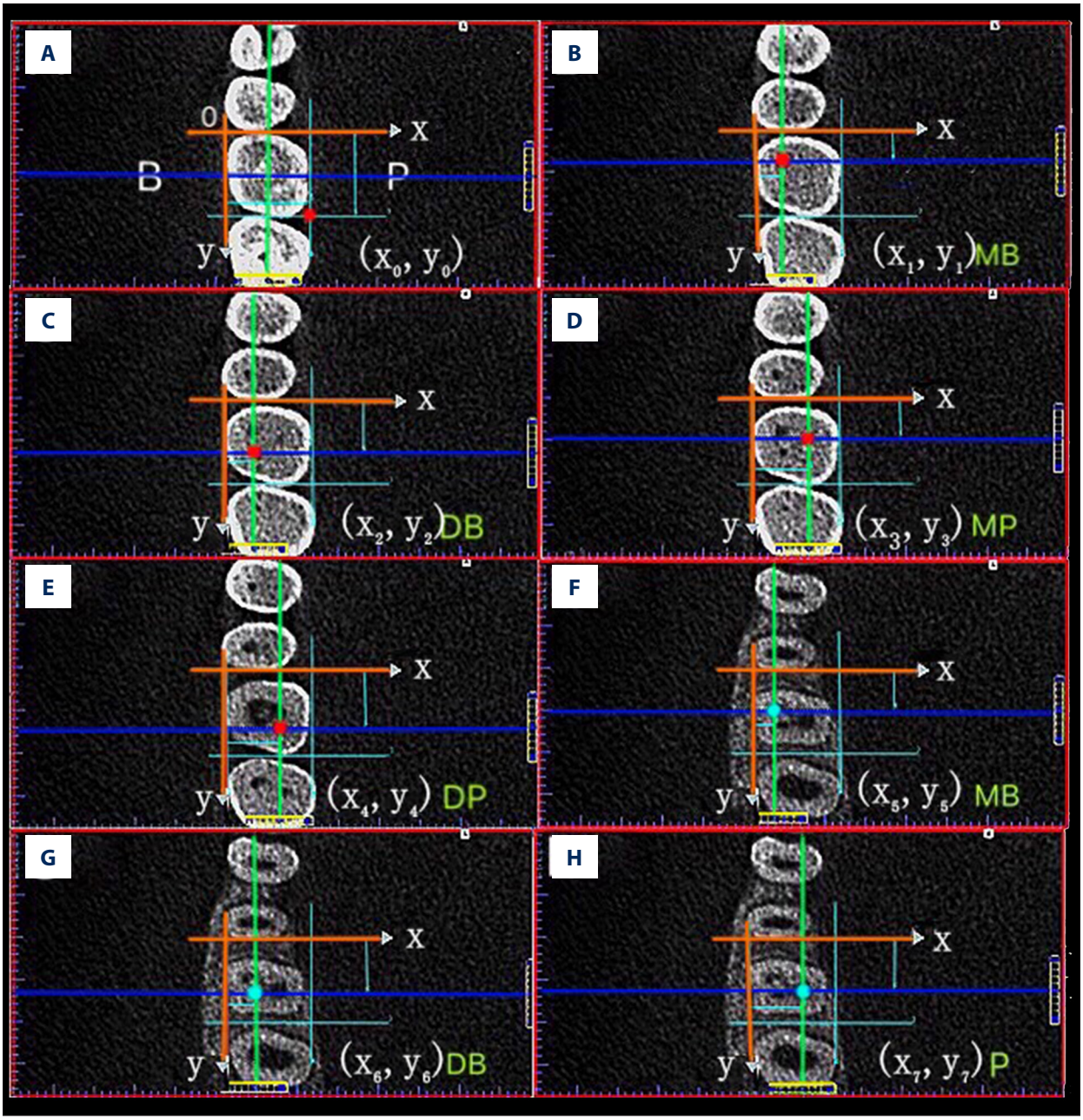


**Figure 2.** Each pulp horn and root canal orifice was identified according to the first appearance of their low-density shadow and was designated by the x, y coordinates in the X and Y axes system. (**A**) Buccal-lingual distance; Mesial-distal distance. (**B-E**) Pulp horns (red dots): the intersection of the coronal plane (blue line) and the sagittal plane (green line) (MB, DB, MP, DB). (**F-H**) Root canal orifices (blue dots): the intersection of the coronal plane (blue line) and the sagittal plane (green line) (MB, DB, P). MB – mesiobuccal; DB – distobuccal; MP – mesiopalatal; DP – distopalatal; P – palatal.





Indexed in: [Current Contents/Clinical Medicine] [SCI Expanded] [ISI Alerting System] [ISI Journals Master List] [Index Medicus/MEDLINE] [EMBASE/Excerpta Medica] [Chemical Abstracts/CAS]

**Table 1.** Symbols used and descriptions of the 16 CBCT measurements.

| Symbols | | Clinical meanings |
|---|---|---|
| $(x_0, y_0)$ | $x_0$ | Buccal-lingual distance: the distance from the buccal marginal ridge to the lingual marginal ridge |
| | $y_0$ | Mesio-distal distance: the distance from the mesial marginal ridge to the distal marginal ridge |
| $(x_1, y_1)$ | $x_1$ | x-Coordinate of MB pulp horn: the distance from the MB pulp horn to the buccal marginal ridge |
| | $y_1$ | y-Coordinate of MB pulp horn: the distance from the MB pulp horn to the mesial marginal ridge |
| $(x_2, y_2)$ | $x_2$ | x-Coordinate of DB pulp horn: the distance from the DB pulp horn to the buccal marginal ridge |
| | $y_2$ | y-Coordinate of DB pulp horn: the distance from the DB pulp horn to the mesial marginal ridge |
| $(x_3, y_3)$ | $x_3$ | x-Coordinate of MP pulp horn: the distance from the MP pulp horn to the buccal marginal ridge |
| | $y_3$ | y-Coordinate of MP pulp horn: the distance from the MP pulp horn to the mesial marginal ridge |
| $(x_4, y_4)$ | $x_4$ | x-Coordinate of DP pulp horn: the distance from the DP pulp horn to the buccal marginal ridge |
| | $y_4$ | y-Coordinate of DP pulp horn: the distance from the DP pulp horn to the mesial marginal ridge |
| $(x_5, y_5)$ | $x_5$ | x-Coordinate of MB orifice: the distance from the MB root canal orifice to the buccal marginal ridge |
| | $y_5$ | y-Coordinate of MB orifice: the distance from the MB root canal orifice to the mesial marginal ridge |
| $(x_6, y_6)$ | $x_6$ | x-Coordinate of DB orifice: the distance from the DB root canal orifice to the buccal marginal ridge |
| | $y_6$ | y-Coordinate of DB orifice: the distance from the DB root canal orifice to the mesial marginal ridge |
| $(x_7, y_7)$ | $x_7$ | x-Coordinate of P orifice: the distance from the P root canal orifice to the buccal marginal ridge |
| | $y_7$ | x-Coordinate of P orifice: the distance from the P root canal orifice to the mesial marginal ridge |

MB – mesiobuccal; DB – distobuccal; MP – mesiopalatal; DP – distopalatal; P – palatal; CBCT – cone-beam computed tomography.

### Data Analysis

Statistical analysis was performed using R software, version 3.5.2 (R Foundation for Statistical Computing; http://www.r-project.org/). Eight coordinate points (8 coordinate points) were analyzed with the Shapiro-Wilk statistical test to assess the normality of data distribution. Levene's test was used to analyze the homogeneity of variance of the 8 coordinate points. Normally distributed data were presented as mean±standard deviation, while skewed data were described using median (upper and lower quartiles). Data satisfying normality and homogeneity of variance assumptions were subjected to an analysis of variance, while the Kruskal-Wallis test was used for data that showed non-normality or inhomogeneity. After grouping by sex, Pearson's correlation test was used to assess the association between the patients' age and the 8 coordinate points. The Kruskal-Wallis test was used to evaluate sex differences for the 8 coordinate points. Significance was set at $P<0.05$.

## Results

The ICC scores between the radiologist and students A and B were 0.98 and 0.97, respectively. The ICC scores of the 2 postgraduates for the first and second time was 0.99 and 0.98, respectively. Therefore, these measurements had high intra- and inter-observer reliability.

Among the 500 CBCT images, 198 were males (39.6%), and 302 were females (60.4%). Age was normally distributed with the mean age being 30.29±12.05 years. The normality tests of the 8 coordinate points are shown in **Table 2**, and those of the homogeneity of variance tests are shown in **Table 3**. No statistically significant correlations were observed between patient age and the 8 coordinate points, either among males or females (**Table 4**).

The nine-rectangle-grid, shown in **Figure 3**, comprised trisection of the buccal-lingual diameter ($L_b$, $L_p$) and trisection of the mesial-distal diameter ($L_m$, $L_d$) on the baseline plane. The projections of 4 pulp horns (red dot) that guide the TEC and 3 root canal orifices (blue dot) that guide the CEC in the baseline plane are shown in **Figure 3A and 3C**. Connecting the 4 red dots formed a red oblique quadrilateral, essentially concentrated in the central area of the nine-rectangle-grid. Similarly, connecting the 3 blue dots formed a blue triangle, primarily in the central grid with extension in the distal and buccal areas (**Figure 3**).

The area of TEC was 9.61 $mm^2$ in males and 8.91 $mm^2$ in females ($P<0.05$, **Table 5**). The area of CEC was 3.4 $mm^2$ in males and 3.16 $mm^2$ in females ($P<0.05$, **Table 5**). The ratio of the





Indexed in: [Current Contents/Clinical Medicine] [SCI Expanded] [ISI Alerting System] [ISI Journals Master List] [Index Medicus/MEDLINE] [EMBASE/Excerpta Medica] [Chemical Abstracts/CAS]

**Table 2.** Shapiro-Wilk normality test of 8 coordinate points for males and females.

| Variable | Men N=198 | | Women N=302 | |
|---|---|---|---|---|
| | W | P-value | W | P-value |
| Age | 0.97 | 0.00 | 0.89 | 0.00* |
| $x_0$ | 0.99 | 0.14 | 0.99 | 0.11 |
| $y_0$ | 0.99 | 0.16 | 0.99 | 0.02* |
| $x_1$ | 0.99 | 0.24 | 0.99 | 0.02* |
| $y_1$ | 0.99 | 0.14 | 0.99 | 0.02* |
| $x_2$ | 0.98 | 0.01* | 0.87 | 0.00* |
| $y_2$ | 0.99 | 0.14 | 0.98 | 0.00* |
| $x_3$ | 0.99 | 0.62 | 0.99 | 0.13 |
| $y_3$ | 0.99 | 0.58 | 0.99 | 0.03* |
| $x_4$ | 0.99 | 0.14 | 0.90 | 0.00* |
| $y_4$ | 0.99 | 0.04* | 0.96 | 0.00* |
| $x_5$ | 0.98 | 0.02* | 0.99 | 0.25 |
| $y_5$ | 0.98 | 0.01* | 0.99 | 0.19 |
| $x_6$ | 0.98 | 0.00* | 0.99 | 0.13 |
| $y_6$ | 0.99 | 0.19 | 0.99 | 0.01* |
| $x_7$ | 0.99 | 0.09 | 0.98 | 0.00* |
| $y_7$ | 0.99 | 0.07 | 1.00 | 0.49 |
| PHPA | 0.99 | 0.21 | 1.00 | 0.76 |
| RCOPA | 0.98 | 0.01* | 0.99 | 0.01* |
| Ratio | 0.89 | 0.00* | 0.89 | 0.00* |

* $P<0.05$. The definitions of $x_0...x_7$, $y_0...y_7$ are shown in Table 1. PHPA – pulp horn projection-connecting lines area; RCOPA – root canal orifice projection-connecting lines area.

**Table 3.** Levene's test for homogeneity of variance of 8 coordinate points for males and females.

| Variable | F | P-value |
|---|---|---|
| Age | 12.95 | 0.00* |
| $x_0$ | 0.10 | 0.75 |
| $y_0$ | 0.13 | 0.71 |
| $x_1$ | 0.11 | 0.74 |
| $y_1$ | 0.00 | 0.95 |
| $x_2$ | 5.43 | 0.02* |
| $y_2$ | 0.50 | 0.48 |
| $x_3$ | 2.50 | 0.11 |
| $y_3$ | 0.05 | 0.82 |
| $x_4$ | 0.05 | 0.82 |
| $y_4$ | 0.03 | 0.87 |
| $x_5$ | 10.11 | 0.00* |
| $y_5$ | 3.29 | 0.07 |
| $x_6$ | 7.97 | 0.00* |
| $y_6$ | 0.43 | 0.51 |
| $x_7$ | 0.11 | 0.74 |
| $y_7$ | 1.00 | 0.32 |
| PHPA | 4.85 | 0.03* |
| RCOPA | 4.75 | 0.03* |
| Ratio | 0.41 | 0.52 |

* $P<0.05$. The definitions of $x_0...x_7$, $y_0...y_7$ are shown in Table 1. PHPA – pulp horn projection-connecting lines area; RCOPA – root canal orifice projection-connecting lines area.

area formed by the pulp horn projection-connecting lines to that of the root canal orifice projection-connecting lines was 2.84 in males and 2.8 in females ($P>0.05$, **Table 5**, **Figure 4**).

## Discussion

In root canal therapy, coronal access preparation is a crucial step and a prerequisite for an excellent endodontic prognosis [22]. Minimally invasive endodontics emphasizes the preservation of a maximal amount of healthy tooth tissue. In the present study, the traditional access cavity was determined by coronal access guided by the projection of the pulp horns. In contrast, the conservative access cavity was determined by coronal access, guided by the projection of the root canal orifices. The location and size of 2 endodontic access cavities were compared based on projections of the pulp horns and the root canal orifices onto the occlusal surface of the right maxillary first molar using CBCT.

The study measurements included a voxel size of 0.25 mm and a large field-of-view for several reasons. First, considering the patient's safety and radiation dose, a small CBCT examination should be considered in cases where lower dose conventional radiography does not provide sufficient information for a confident diagnosis [23]. Second, CBCT is not routinely performed before root canal therapy. It is employed for complex root canal systems when endodontic access cavities have been opened and the roof of the pulp chamber has been removed. Third, the coronal structure is damaged, and dental defects occur when root canal therapy is performed for caries. CBCT images are not suitable for the study of endodontic access cavities. Fourth, it is not ethical to have patients artificially photographed with CBCT with a voxel size of 0.125 mm for conducting the study. It is difficult to obtain such a large sample number of up to 500 CBCT images with intact teeth. Therefore, 500 CBCT images with large field-of-view were obtained when patients visited the hospital for an implant or orthodontic treatment in this study.





Indexed in: [Current Contents/Clinical Medicine] [SCI Expanded] [ISI Alerting System] [ISI Journals Master List] [Index Medicus/MEDLINE] [EMBASE/Excerpta Medica] [Chemical Abstracts/CAS]

**Table 4.** Correlation analysis between age and 8 coordinate points for males and females.

| Variable | Men | | Women | |
|---|---|---|---|---|
| | R | P-value | R | P-value |
| $x_0$ | -0.01 | 1.00 | -0.03 | 1.00 |
| $y_0$ | -0.11 | 1.00 | -0.11 | 1.00 |
| $x_1$ | 0.08 | 1.00 | 0.03 | 1.00 |
| $y_1$ | 0.05 | 1.00 | 0.00 | 1.00 |
| $x_2$ | 0.02 | 1.00 | 0.02 | 1.00 |
| $y_2$ | -0.09 | 1.00 | -0.13 | 0.36 |
| $x_3$ | 0.01 | 1.00 | -0.06 | 1.00 |
| $y_3$ | -0.03 | 1.00 | -0.09 | 1.00 |
| $x_4$ | -0.03 | 1.00 | -0.08 | 1.00 |
| $y_4$ | -0.02 | 1.00 | -0.02 | 1.00 |
| $x_5$ | 0.01 | 1.00 | 0.02 | 1.00 |
| $y_5$ | 0.10 | 1.00 | -0.02 | 1.00 |
| $x_6$ | 0.00 | 1.00 | -0.06 | 1.00 |
| $y_6$ | -0.10 | 1.00 | -0.10 | 1.00 |
| $x_7$ | 0.00 | 1.00 | -0.08 | 1.00 |
| $y_7$ | 0.00 | 1.00 | -0.04 | 1.00 |
| PHPA | -0.08 | 1.00 | -0.15 | 0.22 |
| RCOPA | -0.20 | 0.09 | -0.11 | 1.00 |
| Ratio | 0.14 | 0.93 | -0.01 | 1.00 |

* $P<0.05$. The definitions of $x_0...x_7$, $y_0...y_7$ are shown in Table 1. PHPA – pulp horn projection-connecting lines area; RCOPA – root canal orifice projection-connecting lines area.

For precise measurement, the longitudinal axis of the target tooth was adjusted to be perpendicular to the axial plane (horizontal plane) to obtain the vertical projection point of each pulp horn and root canal orifice on the baseline plane. It was requisite that the center point of the first-appearing, low-density shadow of each pulp horn and root canal orifice on the axial plane view was used, as this would prevent variability (**Figure 2**). Each point was measured 3 times and averaged. Such standardization ensured measurement reproducibility.

However, the $MB_2$ canal orifice was not measured for the following reasons. First, when we initially designed the endodontic access cavity, we considered that the cavity should comply with a minimally invasive treatment strategy. The $MB_2$ canal orifice was not explored before the MB canal orifice was opened by removing the roof of the pulp chamber. Second, it had been reported that an $MB_2$ canal orifice was located 1.25±0.34 mm mesially and 2.68±0.49 mm palatally to the MB canal orifice [24]. Hence, even if an $MB_2$ canal orifice existed, it had little effect on the size of access cavity.

The projection position of the pulp horns and the root canal orifices on the occlusal surface did not change with age (**Table 4**). One explanation is that secondary dentin and pulp calcifications are formed with age. Since secondary dentin is mainly deposited on the pulp chamber walls, the size of the pulp chamber and root canals gradually reduced [25,26]. Pulp calcifications deposit hard tissue on the dentin/pulp interface [27]. Therefore, secondary dentin and pulp calcifications may not affect the position of the pulp horns and the root canal orifices. Another reason there was no difference with age is that the 500 CBCT images were obtained when the patients came to the hospital for an implant or orthodontic treatment. The patients in the study undergoing orthodontic treatment were mostly young (30.29±12.05 years old). Studies with large sample sizes and different age groups should be conducted in future to justify these results.

The connection of the projection of 4 pulp horns formed a quadrilateral, and those of the 3 root canal orifices formed a triangle. The area of TEC was approximately 9.61 $mm^2$ for males and 8.91 $mm^2$ for females, while that of CEC was approximately 3.4 $mm^2$ for males and 3.16 $mm^2$ for females. The dimension of CEC was reduced by 65% compared with straight-line opening access (**Figure 4, Table 5**). This finding may show that in contrast to a straight-line preparation, CEC is less invasive, and can save more dental hard tissue, further decreasing the risk of tooth fracture after treatment. Furthermore, CEC preserves the pulpal chamber roof, allowing distribution of the occlusal forces before reaching the pulpal chamber floor, when the tooth is subjected to high chewing pressure [28].

The baseline plane of the right maxillary first molar was a quadrilateral, composed of a buccal tangent line, palatal tangent line, mesial tangent line, and a distal tangent line. Four trisection lines ($L_m$, $L_d$, $L_b$, $L_p$) formed a nine-rectangle-grid on the baseline plane (**Figure 3**). Interestingly, the projections of pulp horns and root canal orifices were both in the center of the nine-rectangle-grid, except the MB pulp horn and MB canal orifice (**Figure 3**), which were near the center of the nine-rectangle-grid. This finding implies that the distribution of projections can be used as a reference for the design, size, and location of the access cavity in clinical operation. For access, the cavity should be limited to the center of the nine-rectangle-grid, especially for the posterior teeth. Therefore, the concept of a nine-rectangle-grid has an important impact on endodontic access cavities to avoid excessive removal of tooth tissue, correct excessive removal of healthy tooth tissue, and increase the probability of tooth saving, especially for the posterior teeth.

Although the conservative access cavity may preserve more tooth tissue, it compromises the instrumentation of root canals. Further studies are recommended to confirm its effect on the cleaning and shaping of the root canal system. The present study did not use a voxel size of 0.125 mm and a small field-of-view. A





Indexed in: [Current Contents/Clinical Medicine] [SCI Expanded] [ISI Alerting System] [ISI Journals Master List] [Index Medicus/MEDLINE] [EMBASE/Excerpta Medica] [Chemical Abstracts/CAS]

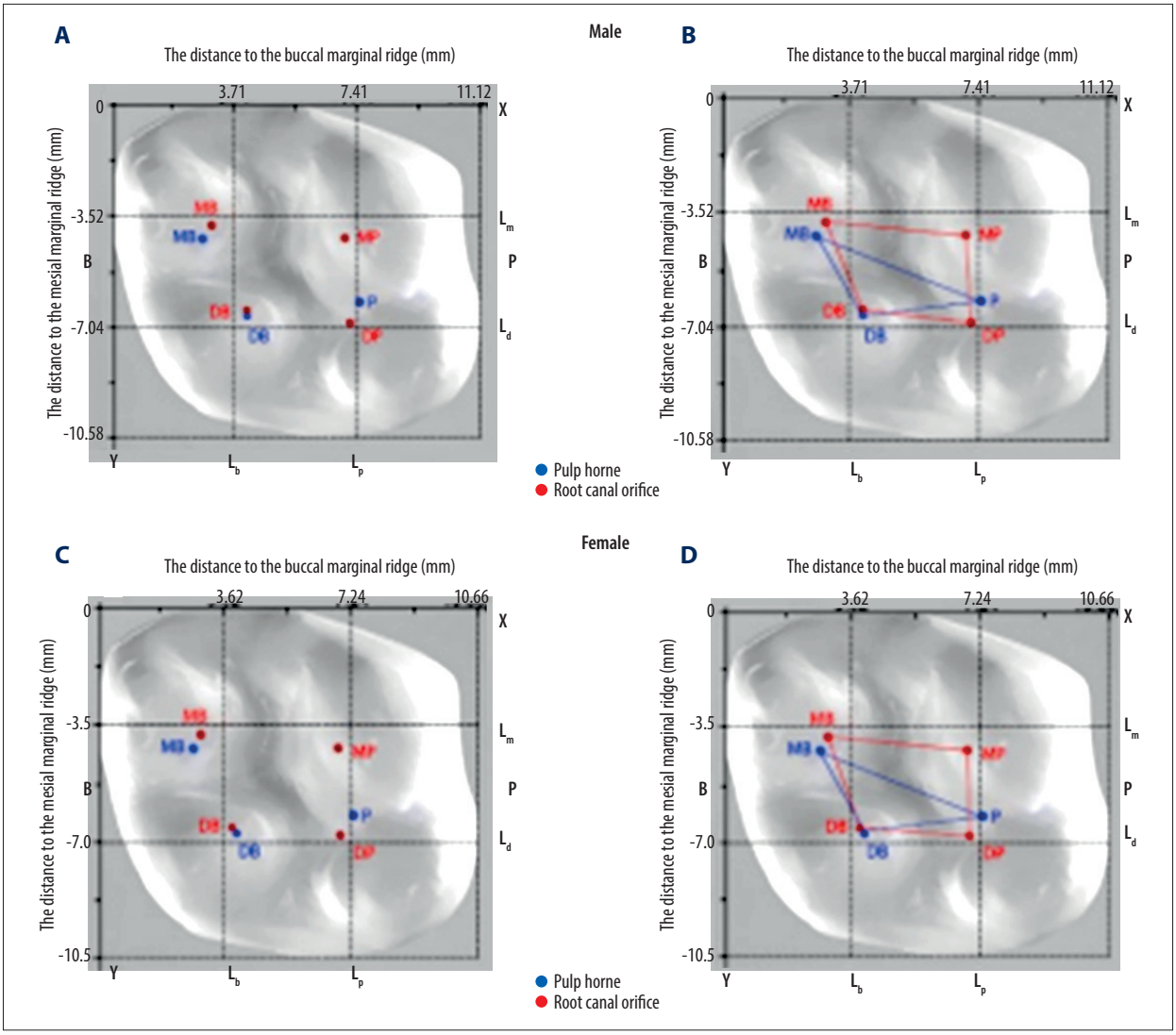


**Figure 3.** Schematic diagram of each anatomical landmark in the nine-rectangle-grid of males and females. (**A**) Distribution of pulp horns (red dot) and root canal orifices (blue dot) in the nine-rectangle-grid in males. (**B**) The blue triangle is the area formed by the root canal orifice projection-connecting lines the red oblique quadrilateral is the area formed by the pulp horn projection-connecting lines in males. (**C**) Distribution of pulp horns (red dot) and root canal orifices (blue dot) in the nine-rectangle-grid in females. (**D**) The blue triangle is the area formed by the root canal orifice projection-connecting lines. The red oblique quadrilateral is the area formed by the pulp horn projection-connecting lines in females. Lb – vertical dotted line near the buccal marginal ridge represents the trisection of the buccal-lingual diameter; Lp – vertical dotted line near the palatal marginal ridge represents the trisection of the buccal-lingual diameter; Lm – horizontal dotted line near the mesial marginal ridge represents the trisection of the mesial-distal diameter; Ld – horizontal dotted line near the distal marginal ridge represents the trisection of the mesial-distal diameter; MB – mesiobuccal; DB – distobuccal; MP – mesiopalatal; DP – distopalatal; P – palatal; TEC – traditional endodontic cavity; CEC – contracted endodontic cavity.





Indexed in: [Current Contents/Clinical Medicine] [SCI Expanded] [ISI Alerting System] [ISI Journals Master List] [Index Medicus/MEDLINE] [EMBASE/Excerpta Medica] [Chemical Abstracts/CAS]

**Table 5.** Single-factor analysis of 8 coordinate points for males and females.

| Variable | Sex | | Statistic | P-value |
|---|---|---|---|---|
| Age (years) | Men | 30.5 (10-43) | 34533 | 0.00* |
| | Women | 26.0 (10-33.75) | | |
| $x_0$ (mm) | Men | 11.12±0.52[a] | 0.1798 | 0.672 |
| | Women | 10.86±0.5[a] | | |
| $y_0$ (mm) | Men | 10.67 (10.33-11)[b] | 15.12 | 0.00* |
| | Women | 10.50 (10.17-10.83)[b] | | |
| $x_1$ (mm) | Men | 3.33 (3.13-3.5)[b] | 6.95 | 0.01* |
| | Women | 3.25 (3.08-3.42)[b] | | |
| $y_1$ (mm) | Men | 3.67 (3.5-3.92)[b] | 6.38 | 0.01* |
| | Women | 3.58 (3.38-3.83)[b] | | |
| $x_2$ (mm) | Men | 3.83 (3.58-4.16)[b] | 14.90 | 0.00* |
| | Women | 3.67 (3.5-3.92)[b] | | |
| $y_2$ (mm) | Men | 6.58 (6.25-6.92)[b] | 19.43 | 0.00* |
| | Women | 6.42 (6.17-6.75)[b] | | |
| $x_3$ (mm) | Men | 7.39±0.52[a] | 2.459 | 0.118 |
| | Women | 7.09±0.47[a] | | |
| $y_3$ (mm) | Men | 7.00 (6.75-7.33)[b] | 16.79 | 0.00* |
| | Women | 6.83 (6.5-7.17)[b] | | |
| $x_4$ (mm) | Men | 7.25 (7-7.56)[b] | 29.21 | 0.00* |
| | Women | 7.08 (6.75-7.33)[b] | | |
| $y_4$ (mm) | Men | 4.63 (4.38-4.92)[b] | 1.13 | 0.29 |
| | Women | 4.58 (4.33-4.91)[b] | | |
| $x_5$ (mm) | Men | 3.04 (2.58-3.38)[b] | 0.23 | 0.64 |
| | Women | 3.00 (2.75-3.33)[b] | | |
| $y_5$ (mm) | Men | 4.75 (4.33-5.17)[b] | 4.81 | 0.03* |
| | Women | 4.66 (4.25-5)[b] | | |
| $x_6$ (mm) | Men | 3.83 (3.5-4.25)[b] | 4.41 | 0.04* |
| | Women | 3.75 (3.5-4.08)[b] | | |
| $y_6$ (mm) | Men | 6.65 (6.33-7)[b] | 16.16 | 0.00* |
| | Women | 6.50 (6.17-6.83)[b] | | |
| $x_7$ (mm) | Men | 7.42 (7.08-7.75)[b] | 36.00 | 0.00* |
| | Women | 7.08 (6.77-7.5)[b] | | |
| $y_7$ (mm) | Men | 6.41±0.53[a] | 0.998 | 0.318 |
| | Women | 6.3±0.48[a] | | |





Indexed in: [Current Contents/Clinical Medicine] [SCI Expanded] [ISI Alerting System] [ISI Journals Master List] [Index Medicus/MEDLINE] [EMBASE/Excerpta Medica] [Chemical Abstracts/CAS]

**Table 5 continued.** Single-factor analysis of 8 coordinate points for males and females.

| Variable | Sex | | Statistic | P-value |
|---|---|---|---|---|
| PHPA (mm²) | Men | 9.61 (8.31-11.18)[b] | 19.79 | 0.00* |
| | Women | 8.91 (7.85-10.29)[b] | | |
| RCOPA (mm²) | Men | 3.40 (2.78-4.27)[b] | 11.03 | 0.00* |
| | Women | 3.16 (2.5-3.82)[b] | | |
| Ratio | Men | 2.84 (2.28-3.48)[b] | 0.02 | 0.88 |
| | Women | 2.80 (2.31-3.43)[b] | | |

[a] ANOVA; [b] Kruskal-Wallis. * P<0.05. The definitions of $x_0...x_7$, $y_0...y_7$ are shown in Table 1. PHPA – pulp horn projection-connecting lines area; RCOPA – root canal orifice projection-connecting lines area.

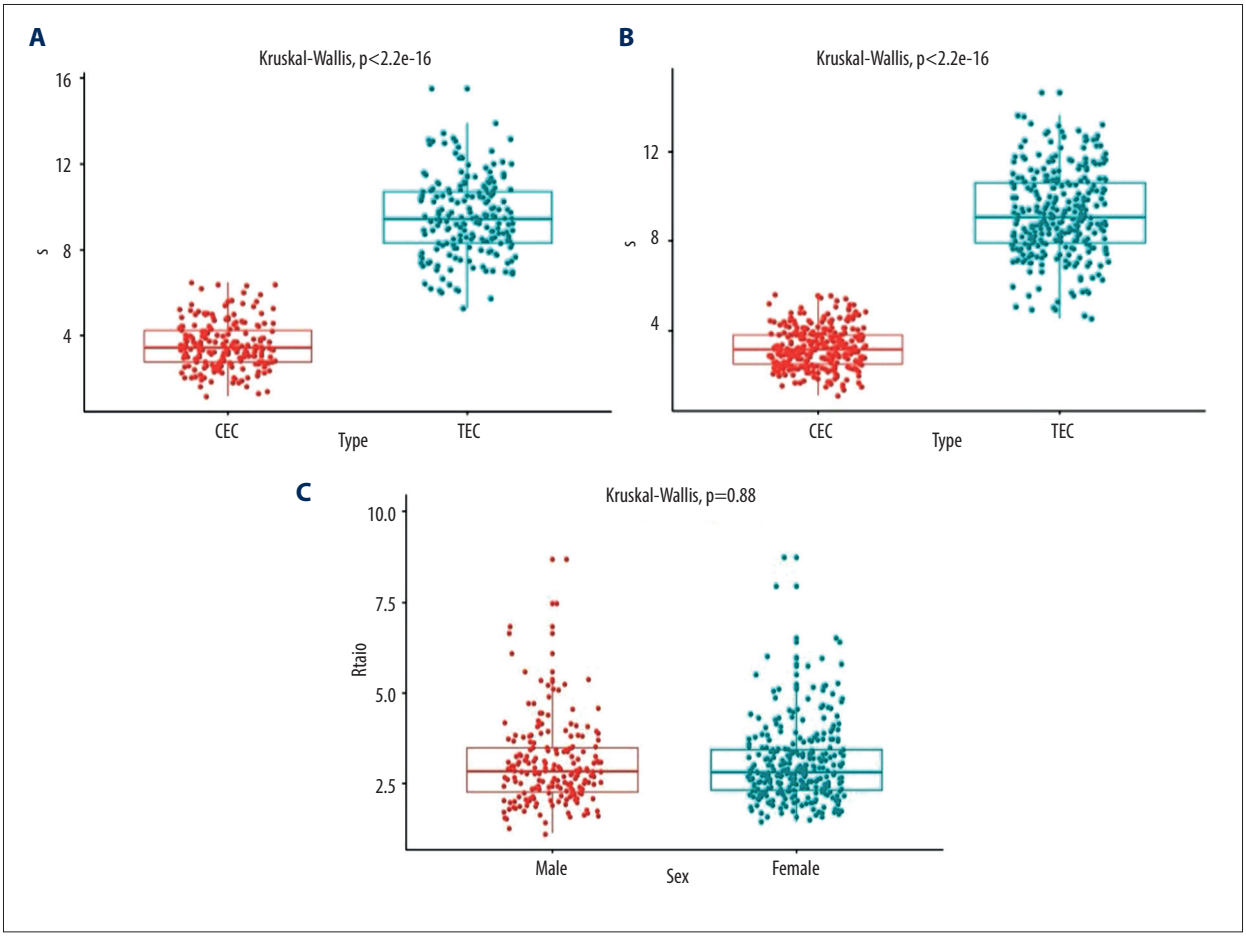


**Figure 4.** Analysis of differences in RCOPA and PHPA in males and females. (**A**) Comparative analysis of the area of RCOPA and PHPA in males (n=198). (**B**) Comparative analysis of the area of RCOPA and PHPA in females (n=302). (**C**) Comparative analysis of the ratio of PHPA to RCOPA between males and females. PHPA – pulp horn projection-connecting lines area; RCOPA – root canal orifice projection-connecting lines area.





Indexed in: [Current Contents/Clinical Medicine] [SCI Expanded] [ISI Alerting System] [ISI Journals Master List] [Index Medicus/MEDLINE] [EMBASE/Excerpta Medica] [Chemical Abstracts/CAS]

future study should be performed with micro-computed tomography to provide useful information with higher quality images.

## Conclusions

The CEC is less invasive than the TEC. The concept of nine-rectangle-grid can be used as a guide for clinical access opening, especially for posterior teeth.

### Acknowledgements

We would like to thank all members for their contributions to the completion of this article, and thank Mrs. Wu for her guidance, review and supervision. We also express sincere thanks to the Research Plan of Undergraduate Teaching Quality and Teaching Reform in Tianjin Ordinary Colleges and Universities for its support.

### Conflicts of Interest

None.

### Declaration of Figures Authenticity

All figures submitted have been created by the authors who confirm that the images are original with no duplication and have not been previously published in whole or in part.

## References:

1. Yuan K, Niu C, Xie Q, et al. Comparative evaluation of the impact of minimally invasive preparation vs. conventional straight-line preparation on tooth biomechanics: A finite element analysis. Eur J Oral Sci. 2016;124:591-96
2. Krishan R, Paque F, Ossareh A, et al. Impacts of conservative endodontic cavity on root canal instrumentation efficacy and resistance to fracture assessed in incisors, premolars, and molars. J Endod. 2014;40:1160-66
3. Tang W, Wu Y, Smales RJ. Identifying and reducing risks for potential fractures in endodontically treated teeth. J Endod. 2010;36:609-17
4. Sedgley CM, Messer HH. Are endodontically treated teeth more brittle? J Endod. 1992;18:332-35
5. Sabeti M, Kazem M, Dianat O, et al. Impact of access cavity design and root canal taper on fracture resistance of endodontically treated teeth: An ex vivo investigation. J Endod. 2018;44:1402-6
6. Patel S, Rhodes J. A practical guide to endodontic access cavity preparation in molar teeth. Br Dent J. 2007;203:133-40
7. Reeh ES, Messer HH, Douglas WH. Reduction in tooth stiffness as a result of endodontic and restorative procedures. J Endod. 1989;15:512-16
8. Gluskin AH, Peters CI, Peters OA. Minimally invasive endodontics: Challenging prevailing paradigms. Br Dent J. 2014;216:347-53
9. Clark D, Khademi J. Modern molar endodontic access and directed dentin conservation. Dent Clin North Am. 2010;54:249-73
10. Clark D, Khademi JA. Case studies in modern molar endodontic access and directed dentin conservation. Dent Clin North Am. 2010;54:275-89
11. Burklein S, Schafer E. Minimally invasive endodontics. Quintessence Int. 2015;46:119-24
12. Eaton JA, Clement DJ, Lloyd A, Marchesan MA. Micro-computed tomographic evaluation of the influence of root canal system landmarks on access outline forms and canal curvatures in mandibular molars. J Endod. 2015;41:1888-91
13. Moore B, Verdelis K, Kishen A, et al. Impacts of contracted endodontic cavities on instrumentation efficacy and biomechanical responses in maxillary molars. J Endod. 2016;42:1779-83
14. Gorduysus O, Nagas E, Cehreli ZC, et al. Localization of root canal orifices in mandibular second molars in relation to occlusal dimension. Int Endod J. 2009;42:973-77
15. Kirkevang LL, Horsted-Bindslev P, Orstavik D, Wenzel A. Frequency and distribution of endodontically treated teeth and apical periodontitis in an urban Danish population. Int Endod J. 2001;34:198-205
16. Su C-C, Huang R-Y, Wu Y-C, et al. Detection and location of second mesiobuccal canal in permanent maxillary teeth: A cone-beam computed tomography analysis in a Taiwanese population. Arch Oral Biol. 2019;98:108-14
17. Neelakantan P, Subbarao C, Ahuja R, et al. Cone-beam computed tomography study of root and canal morphology of maxillary first and second molars in an Indian population. J Endod. 2010;36:1622-27
18. Rocca GT, Saratti CM, Cattani-Lorente M, et al. The effect of a fiber reinforced cavity configuration on load bearing capacity and failure mode of endodontically treated molars restored with CAD/CAM resin composite overlay restorations. J Dent. 2015;43:1106-15
19. Tian XM, Yang XW, Qian L, et al. Analysis of the root and canal morphologies in maxillary first and second molars in a Chinese population using cone-beam computed tomography. J Endod. 2016;42:696-701
20. Ratanajirasut R, Panichuttra A, Panmekiate S. A cone-beam computed tomographic study of root and canal morphology of maxillary first and second permanent molars in a thai population. J Endod. 2018;44:56-61
21. Azim AA, Azim KA, Deutsch AS, Huang GT. Acquisition of anatomic parameters concerning molar pulp chamber landmarks using cone-beam computed tomography. J Endod. 2014;40:1298-302
22. Zhang Y, Xu H, Wang D, et al. Assessment of the second mesiobuccal root canal in maxillary first molars: A cone-beam computed tomographic study. J Endod. 2017;43:1990-96
23. Patel S, Brown J, Semper M, et al. European Society of Endodontology position statement: Use of cone beam computed tomography in Endodontics European Society of Endodontology (ESE) developed by. Int Endod J. 2019;52:1675-78
24. Azim AA, Azim KA, Deutsch AS, Huang GTJ. Acquisition of anatomic parameters concerning molar pulp chamber landmarks using cone-beam computed tomography. J Endod. 2014;40:1298-302
25. Gani O, Visvisian C. Apical canal diameter in the first upper molar at various ages. J Endod 1999;25:689-91
26. Stanley HR, White CL, McCray L. The rate of tertiary (reparative) dentine formation in the human tooth. Oral Surg Oral Med Oral Pathol. 1966;21:180-89
27. Carvalho TS, Lussi A. Age-related morphological, histological and functional changes in teeth. J Oral Rehabil. 2017;44:291-98
28. Ozyurek T, Ulker O, Demiryurek EO, Yilmaz F. The effects of endodontic access cavity preparation design on the fracture strength of endodontically treated teeth: Traditional versus conservative preparation. J Endod. 2018;44:800-5





Indexed in: [Current Contents/Clinical Medicine] [SCI Expanded] [ISI Alerting System] [ISI Journals Master List] [Index Medicus/MEDLINE] [EMBASE/Excerpta Medica] [Chemical Abstracts/CAS]